Mechanism of Alloying Element Vaporization during Laser Welding

M. M. COLLUR, A. PAUL, and T. DEBROY

Vaporization of alloying elements is a serious problem in the laser welding of many important engineering alloys. Since the available mass transfer correlations are not applicable for credible assessment of the rates of transport of vaporized species in the gas phase, the role of gas phase mass transfer in the overall vaporization of alloying elements was examined by conducting several critical experiments. The rates of transport of alloying elements in the weld pool were determined from numerically computed fluid flow fields. Since the weld pool is surrounded by plasma during laser welding, the role of plasma in the vaporization of alloying elements was physically modeled by allowing molten copper drops to vaporize isothermally both in the presence and absence of plasma. The transport of alloying elements in both liquid and gas phases was found to be rapid and the overall vaporization rates were controlled by the plasma influenced intrinsic vaporization of alloying elements at the weld pool surface. The experimentally obtained rates of vaporization of alloying elements from laser melted stainless steel weld pools were compared with the corresponding theoretically calculated values.

I. INTRODUCTION

DURING laser welding, the use of a high power laser beam focused to a very small area leads to relatively high weld pool temperatures and significant vaporization of volatile elements. The loss of volatile components results in a change in the composition of the weldment, affects weld properties, and is a serious problem in the fabrication of many important engineering alloys.[1-6] For example, laser welding of Al-Mg alloys resulted in significant loss of magnesium and excessive porosity of the weldments.[1] Similarly, butt welding of thick plates of aluminum alloy 5456 containing 5.25 wt pct magnesium, by a high power (8 kW) carbon dioxide gas laser resulted in significant degradation of the mechanical properties due to the loss of magnesium.[2] Changes in the concentration of alloying elements in the laser irradiated zone of alloy steels and stainless steels were reported by several investigators.[5,6] The severe depletion in the concentration of manganese in the weld zone of three grades of high manganese stainless steels determined by electron probe microanalysis is shown in Figure 1. Although significant changes in the chemical composition and the properties of the weld metal were recognized in the earlier work, the emphasis in the past work was on the characterization of the final product and not on the fundamental mechanism of vaporization on which improved control of chemical composition and properties of the fabricated product can be based.

The vaporization of alloying elements during welding is a complex process which can be broadly subdivided into three steps. The first step involves the transport of the alloying elements from the interior to the surface of the weld pool aided by the fluid motion in the weld pool.[7] Secondly, once the alloying element reaches the surface of the weld pool,

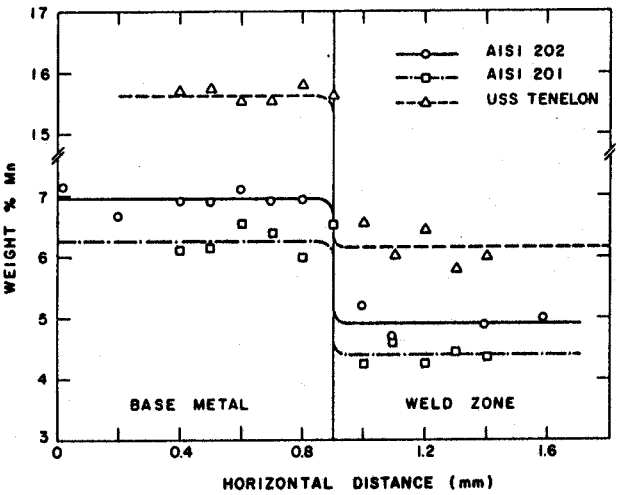

Fig. 1—Concentration profile of manganese in the weld zone and base metal for AISI 201, AISI 202, and USS Tenelon stainless steels. Laser power: 560 watts, welding speed: 3.5×10^{-3} m/s, shielding gas flow rate: 1×10^{-4} m^3/s, and sample thickness: 7×10^{-4} m.

the rate of vaporization is determined by the surface temperature distribution, local concentration of the alloying element, the extent of surface coverage by the surface active elements, and by other factors such as the surface agitation and modification of the nature of the interface due to the presence of plasma in the vicinity of the weld pool. Finally, the rate of transport of the vaporized alloying elements from the weld pool surface to the bulk gas phase depends on the nature of the boundary layer and the diffusivities of the vaporized species. The mechanism of vaporization depends on the relative contributions of these three steps in the overall rate of alloying element vaporization. A knowledge of the vaporization mechanism is essential in providing a basis for achieving a better control of the composition of the weldment.

M. M. COLLUR and A. PAUL, Graduate Students, and T. DEBROY, Associate Professor of Metallurgy, are with the Department of Materials Science and Engineering, The Pennsylvania State University, University Park, PA 16802.

Manuscript submitted January 2, 1987.

In many well-defined flow systems, the gas phase mass transfer rates can be estimated from the appropriate mass transfer correlations available in the literature. In laser welding, inherent complexities such as the presence of excited neutral atoms and ionized species in the plasma and their interactions with the laser beam preclude the application of the existing mass transfer correlations. Therefore, the strategy adopted in the current work to assess the role of gas phase mass transfer in the overall vaporization rate was based on the results of a series of critical experiments. In these experiments provision was made for altering the gas phase mass transfer rates to observe the effect of this change on the overall vaporization rate. Both the nature and the flow rate of the shielding gas were changed for this purpose. The examination of the role of transport in the liquid phase was based on the computed fluid flow field. Furthermore, the concentration profile of nitrogen in the rapidly solidified laser melted weld pools obtained by secondary ion mass spectrometry was examined. Unlike the transport of elements in the liquid phase, the intrinsic rate of vaporization at the interface is complex because of the presence of plasma above the weld pool and the presence of surface active species. In the rate data obtained by laser welding experiments, the effect of plasma on the overall vaporization rate is masked by the effects of several factors such as the laser beam absorption, weld pool surface temperature profile, and the extent of melting (surface area for vaporization). In this study, the role of plasma on the kinetics of vaporization rate was physically simulated by conducting isothermal experiments with pure copper both in the presence and absence of plasma.

II. EXPERIMENTAL

A high manganese stainless steel, AISI 201 (mole fractions of Fe, Mn, Cr, and Ni were 0.69, 0.065, 0.18, and 0.042, respectively) was laser irradiated by a carbon dioxide laser, Coherent Model Everlase 525-1, capable of producing a maximum output power of 575 watts in the continuous wave mode. Samples were placed on a computer controlled table capable of providing motion in two mutually perpendicular directions along the horizontal plane. All welding was carried out inside a plexiglass box under inert atmosphere using a 2.54×10^{-2} m diameter, 0.127 m focal length Zn-Se lens with an antireflection coating.

The total rate of alloying element vaporization was determined from the measured values of the loss in sample weight resulting from element vaporization and the laser material interaction time.

The role of plasma on the rate of vaporization of copper was studied under isothermal conditions by using an experimental set-up shown in Figure 2. About 5×10^{-4} Kg of electrolytic grade copper (99.9 wt pct Cu, 550 ppm O, 30 ppm S) was placed on an alumina substrate inside a long vycor tube which was filled with ultra high purity argon or helium at a predetermined pressure. The sample was heated by means of an induction coil connected to a 10 kW radio frequency generator. The temperature of the droplet was monitored by means of a two-color pyrometer through an optical grade window fitted at one end of the vycor tube. No condensation of vapors was observed on the window. The low pressure inert gas plasma was characterized by emission

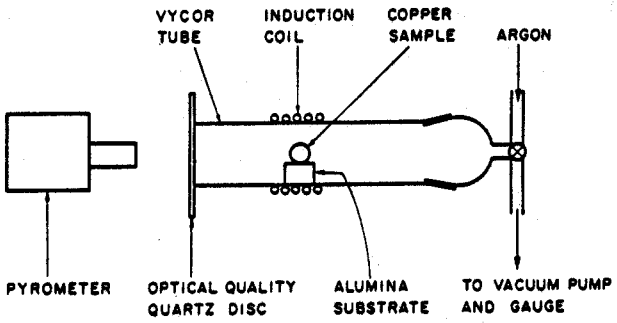

Fig. 2—A schematic diagram of the experimental set-up used for isothermal vaporization experiments with copper at reduced inert gas pressures.

spectroscopy. From the spectra obtained, it was found that the plasma contained both excited neutral and ionized argon species. The intensity of the various peaks of the spectra could be controlled by varying the input power (current) and the chamber pressure. At a predetermined plasma intensity, the temperature of the droplet was controlled by adjusting the position of the droplet with respect to the induction coil. The copper vaporization rate was determined from the weight loss of the sample and the duration of the experiments.

III. RESULTS AND DISCUSSION

A. *Mass Transfer in the Liquid Phase*

Transport of alloying elements in the weld pool is affected by the circulation of molten liquid resulting from the spatial variation of surface tension due to the existence of a strong temperature gradient at the surface of the weld pool. A velocity vector plot of the flow pattern in the weld pool obtained by the simultaneous solutions of the equations of change is given in Figure 3. Details of this computation are given elsewhere.[13] A packet of hot metal traveling at a velocity of 0.50 m/s would require only about 0.0006 seconds to traverse a weld pool half width of 0.03 cm. This is two orders of magnitude smaller than the 0.12 seconds that is required for the laser beam to scan the 0.06 cm length of the weld pool at a welding speed of 0.5×10^{-2} m/s. It is clear that the weld pool surface can be renewed about two

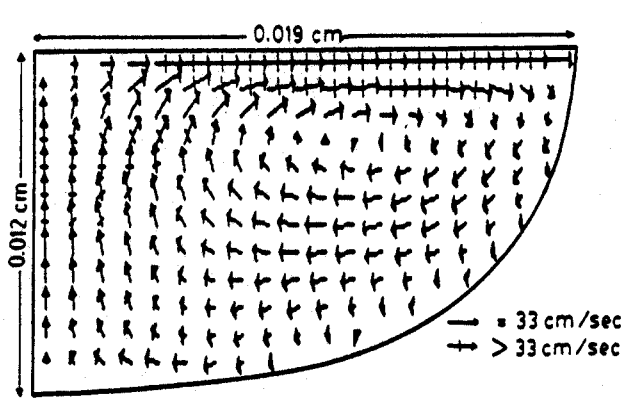

Fig. 3—Computed velocity field in the vertical plane perpendicular to the welding direction. Material: pure iron and laser power: 500 watts.

hundred times in the time period required for the laser beam to scan a distance equal to the weld pool width. Therefore, the liquid phase is considered very well mixed and the transport in the liquid phase does not inhibit vaporization.

An additional evidence of rapid liquid phase mass transport was obtained by Khan and DebRoy[8] who determined the concentration profile of nitrogen starting from the surface of the rapidly solidified weld pool traversing downward along the depth by secondary ion mass spectrometry. Their data do not indicate the existence of a concentration variation near the surface of the weld pool characteristic of liquid phase mass transfer controlled vaporization. Since the loss of nitrogen is quite pronounced during welding, the absence of variation of the concentration of nitrogen near the surface is again a testimony of rapid liquid phase transport.

B. *Role of Gas Phase Mass Transfer*

If the gas phase mass transfer is the rate controlling step in the overall vaporization process, the diffusivities of the vaporizing species (*e.g.*, manganese) in the shielding gas (*e.g.*, helium) should have an effect on the vaporization rate. Furthermore, since the flow rate of the shielding gas influences the mass transfer coefficient, its change is also expected to have an influence on the rate if the rate is gas phase mass transfer controlled. The diffusivities of manganese and iron vapors in argon, helium, and nitrogen at various temperatures, calculated on the basis of Chapman-Enskog theory,[9] are presented in Table I. It is clear from the table that the diffusivity of manganese in helium is about four times that in argon or nitrogen. Similar observation can be made for iron. With this in view, the rates of vaporization of alloying elements from AISI 201 stainless steel were experimentally measured using various shielding gases and flow rates. Figure 4 depicts the results of these experiments. It may be noted that the vaporization rate is insensitive to changes in the diffusivity of the vaporizing species (shielding gas type) and flow rate, indicating that the gas phase mass transfer step does not contribute significantly to the overall vaporization rate.

C. *Vaporization at the Weld Pool Surface*

From the discussions in the previous sections, it is clear that the resistances offered by the liquid phase and gas phase transports in the overall vaporization of alloying elements are insignificant and the slowest step is the vaporization reaction at the weld pool surface. The vaporization flux for species i from a clean weld pool surface at low pressure is given by the following equation:[10]

$$J_i(T) = 44.34 \frac{P_i(T)}{\sqrt{M_i T}} \qquad [1]$$

Table I. Diffusivities of Manganese and Iron Vapors in Various Gases $\times 10^4$, m^2/s

	Manganese (g)			Iron (g)		
T (K)	He	N_2	Ar	He	N_2	Ar
1800	15.85	3.96	3.71	15.84	3.78	3.62
2100	19.97	5.29	4.89	19.96	4.98	4.66
2500	25.94	7.13	6.65	25.92	6.78	6.40
3100	35.82	9.97	9.75	35.80	9.94	9.48

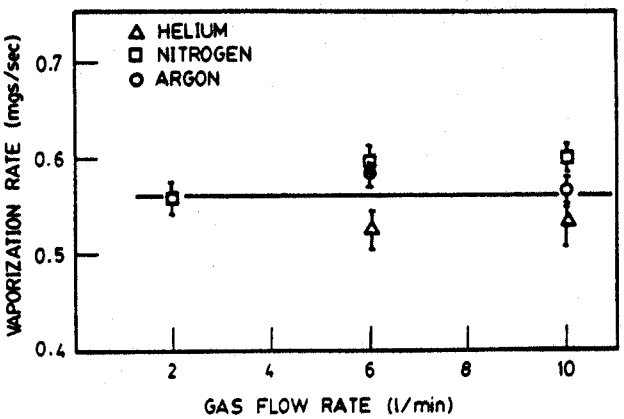

Fig. 4 — Variation of vaporization rate of AISI 201 steel as a function of gas flow rate for various shielding gases. Laser power: 540 watts, welding speed = 5×10^{-3} m/s, and sample thickness = 1.2×10^{-3} m.

All symbols are explained at the end of the text.

The vaporization rate for a component i can be obtained by integrating the local vaporization fluxes given by Eq. [1] over the weld pool surface. The overall vaporization rate is obtained by adding the individual vaporization rates of the various varporizing species. This calculation procedure would be valid only for ultra high purity alloys that do not contain surface active impurities such as sulfur and oxygen. However, since most real materials almost inevitably contain small concentrations of surface active impurities, a portion of the sites is not available for vaporization due to segregation of these impurities on the surface. It was noted earlier that the weld pool surface is renewed rapidly during welding. The rapid circulation in the weld pool and the resulting surface renewal can potentially diminish the extent of surface segregation. However, if the surface segregation rates are very rapid, it is conceivable that despite rapid surface renewal a significant portion of the surface sites can be covered by impurities. Since the data on the rates of surface segregation are not available in the literature, an assessment of the role of surface renewal in the reduction of surface segregation cannot be made.

In view of the foregoing, two extreme cases were considered. In the first case the surface renewal rates were assumed to be dominant and in the second case the surface segregation rates were regarded as dominant. In the former case of mixing dominated system no significant segregation of surface active impurities occurs and the local vaporization flux is given by Eq. [1]. The surface temperature profiles obtained numerically from the solution of the equations of continuity, momentum, and energy[13] were used to calculate the total vaporization rate. Representing the surface of the weld pool approximately by a circle of radius r, the vaporization rate $\dot{v}$ is given by the following equation:

$$\dot{v} = \sum_{\text{elements}} \int_0^r 2\pi J_i(T) r \, dr \qquad [2]$$

Vaporization rates of various alloying elements were computed as a function of the radial distance. For these calculations, equilibrium vapor pressures over pure liquid iron,[11] manganese,[11,12] chromium and nickel[11] were obtained from the literature and the data are presented in the appendix. The partial pressure values over the liquid stainless steel

appearing in Eq. [1] were obtained by multiplying the equilibrium vapor pressure values with the mole fractions of the corresponding elements. The temperature distributions obtained numerically[7] at various laser powers[13] are presented in Figure 5. Using the temperature distribution at the surface of the weld pool when 500 watts of laser power was used, the computed values of the vaporization flux are presented in Figure 6 as a function of distance from the axis of the laser beam. Similar calculations were performed for welding at various other laser powers. These calculated rates along with the experimentally observed vaporization rates (all elements taken together) are plotted as a function of laser power in Figure 7. It may be noted that the calculated rates are significantly higher than the experimentally determined values.

In the second case, when the surface segregation rates were assumed to be much faster than the surface renewal rates, the fraction of surface sites occupied by a surface active element, θ, was calculated on the basis of adsorption considerations. The fraction of occupied surface sites is a function of temperature and therefore it varies radially. The amount of surface coverage due to the presence of surface active impurities can be estimated from the variation of the surface tension with the concentration of various impurities in the alloy as described in the appendix. From this analysis, the calculated values of a fraction of surface sites occupied

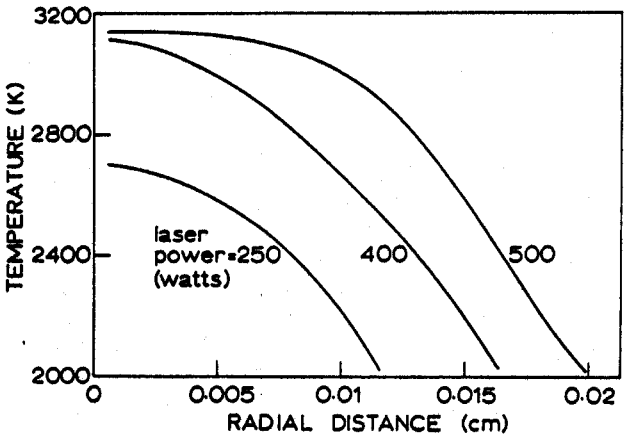

Fig. 5—Radial variation of temperature at various laser powers.[13]

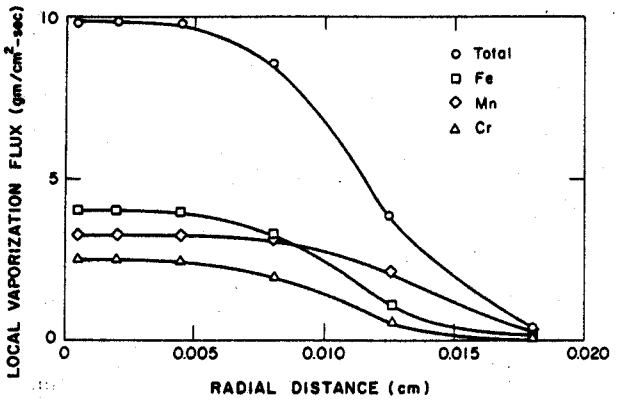

Fig. 6—Vaporization flux of alloying elements calculated from the Langmuir-Knudsen equation (Eq. [1]).

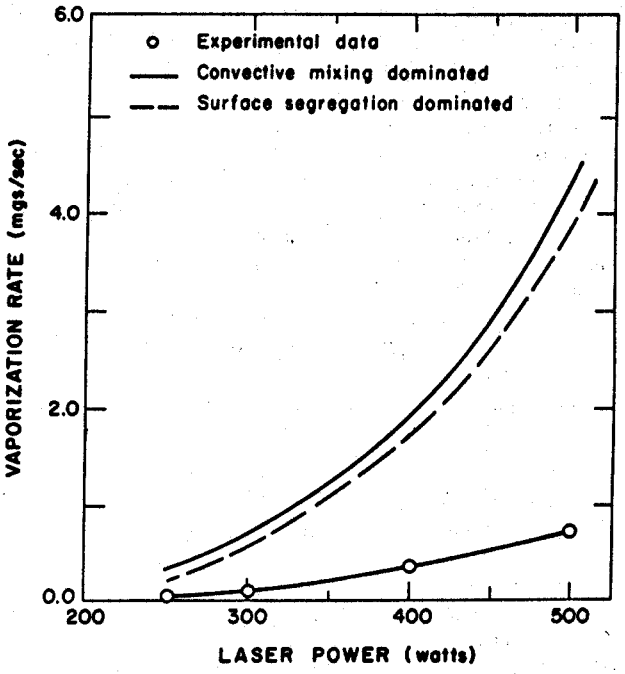

Fig. 7—Comparison of experimental vaporization rates with the calculated vaporization rates for convective mixing dominated and surface segregation dominated systems at various laser powers. Welding speed: 3.5×10^{-3} m/s, shielding gas flow rate: 1×10^{-4} m^3/s, and sample thickness: 7×10^{-4} m.

by sulfur and oxygen are plotted as a function of temperature in Figure 8. The total vaporization rate was calculated utilizing these local values of θ (from Figure 8), corresponding to the sulfur and oxygen contents of AISI 201 stainless steel (0.004 wt pct S and 0.004 wt pct O), by using the following equation:

$$\dot{v} = \sum_{\text{elements}} \int_0^r 2\pi[1 - \theta(T)]J_i(T)r\,dr \qquad [3]$$

The calculated vaporization rate is plotted as a function of laser power in Figure 7 (dashed line). It is observed from this figure that the theoretically calculated vaporization rates are substantially higher than the vaporization rate determined experimentally. However, in these calculations the effect of plasma (which is inevitably present above the weld pool during laser welding) was ignored.

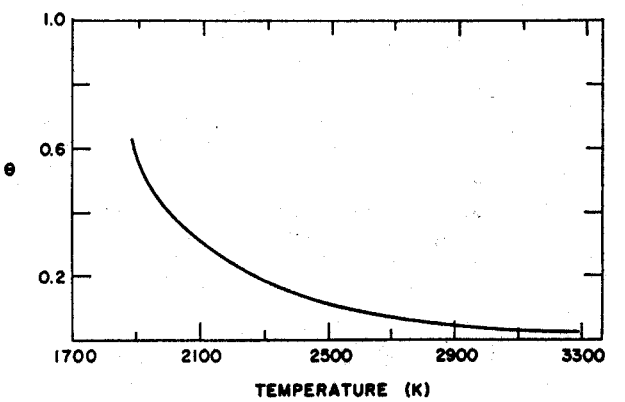

Fig. 8—Fraction of surface sites covered, θ, *vs* temperature for iron-oxygen-sulfur system.

D. *Effect of Plasma on the Vaporization Rate*

To determine the effect of plasma on the vaporization rate, vaporization rates of pure copper samples were determined under reduced pressure with and without the presence of plasma. The results of these experiments are plotted in Figure 9. In experiments with plasma, the plasma intensity was maintained constant by keeping the coil configuration, coil current, and the chamber pressure of argon (210 μ Hg) constant[14] at all temperatures. It is observed from this figure that the vaporization flux is decreased significantly when plasma is present. This effect could be due to one of the following two reasons or a combination of both. First, since the argon atoms are ionized, as indicated from emission spectroscopy data,[14] the copper atoms which have a much lower ionization potential (7.72 ev) as compared to argon (15.75 ev) are also ionized. Because of the electrical repulsion of the positively charged argon cloud in close proximity to the vaporizing interface, the recondensation of the copper on the liquid surface is favored as depicted in Figure 10(a). Second, the surface active elements such as sulfur and oxygen, which are negatively charged due to the formation of ionic double layers,[15,16] should have an enhanced tendency of segregating to the surface due to the electrical attraction from the positively charged cloud of metallic and shielding gas species as shown in Figure 10(b). This mechanism could result in an increased surface coverage and a consequent decrease in the vaporization flux.

In order to determine if the variation of the intensity of the plasma has an effect on vaporization flux, experiments were conducted under different intensities of the plasma. The plasma intensity was varied by changing the pressure in the reaction chamber. Figure 11 depicts the results of these experiments. Above a gas pressure of about 200 microns of Hg, which was the minimum pressure required to sustain a stable plasma, no significant change was observed in the vaporization flux. It seems that in the presence of a positively charged cloud, the enhanced surface segregation of the negatively charged surface active species such as sulfur and oxygen reaches a saturation beyond which no further surface coverage is possible.

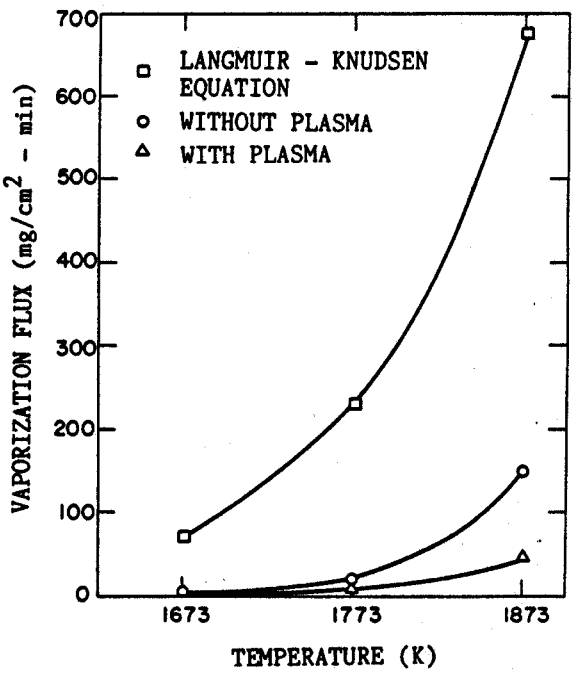

Fig. 9—Comparison between the theoretical vaporization flux calculated from the Langmuir-Knudsen equation (Eq. [1]) and the experimental vaporization flux of copper (in the presence and absence of plasma).

It should be noted that under the conditions of these experiments, the vaporization flux was indeed controlled by the intrinsic vaporization at the liquid surface and the decrease in the vaporization flux observed in Figure 9 is a true effect of the presence of plasma, and is not influenced by the effect of gas phase mass transfer. Since the molecular diffusivity is inversely proportional to pressure, the diffusivity of the copper vapors in the inert gas was enhanced by several orders of magnitude over the diffusivity at atmospheric pressure. This results in a significant increase in the gas phase mass transport rates. Figure 12 represents the variation of the vaporization flux as a function of pressure in the reaction chamber when either argon or helium was used as the atmosphere above the copper droplet at 1773 K. In all these experiments, the pressure was maintained sufficiently low to avoid the formation of plasma. It is clear that the vaporization flux is not a strong function of either the pressure or the type of gas used. These data therefore confirm that the vaporization from the pure copper droplet was not controlled by mass transfer in the gas phase and the rate was controlled by intrinsic vaporization at the surface.

If the entire surface of the copper drop is available for vaporization and no significant segregation of oxygen and sulfur at the surface is assumed, the vaporization flux determined experimentally at various temperatures should be in agreement with the vaporization flux predicted by Eq. [1]. Figure 9 shows both the calculated and the experimentally determined vaporization fluxes as a function of temperature. It is clear that the vaporization fluxes calculated assuming no surface segregation are significantly higher than the experimental fluxes. If the surface segregation rates are assumed to be significantly faster than the surface renewal rates, the lower value of the experimentally determined flux can be attributed to the partial coverage of the surface of the copper drop by oxygen and sulfur. In such a case, the ratio of the experimentally determined vaporization flux in the absence of plasma and the theoretically calculated vaporization flux using Eq. [1] is equal to the fraction of surface sites available for vaporization, *i.e.*, the fraction of sites not covered by oxygen or sulfur, $(1-\theta)$. The values of θ were determined for the isothermal vaporization of copper drops at various temperatures using the ratio of the vaporization fluxes presented in Figure 9. The values of θ thus obtained are shown in Figure 13. The values of the fraction of surface sites occupied by sulfur and oxygen were also estimated from adsorption considerations as described in the appendix. The estimated values are presented in Figure 13 as a solid line. It is observed from this figure that the values of θ obtained by the two procedures are in fair agreement, indicating that small amounts of sulfur and oxygen present in the copper droplet can suppress the vaporization rate to a large extent.

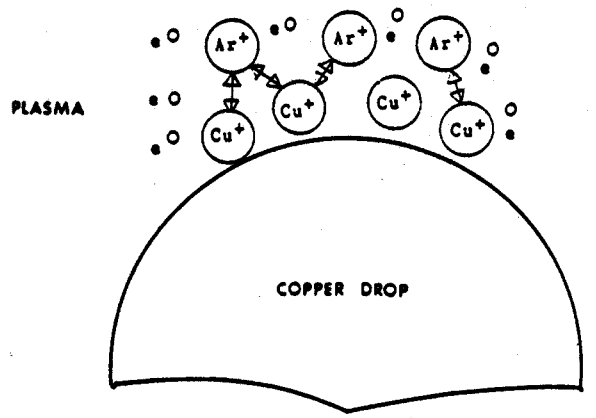

(*a*)

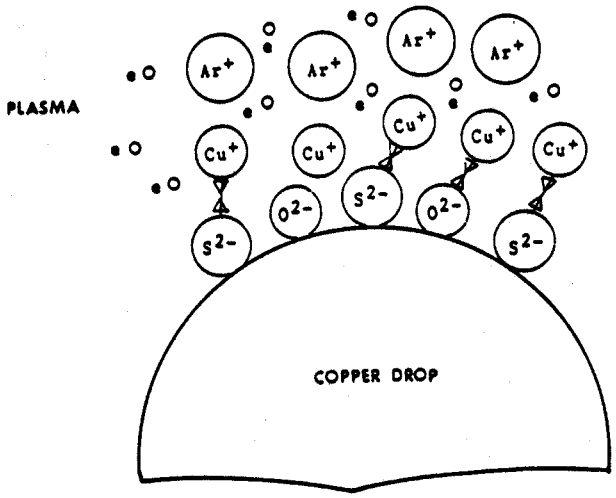

(*b*)

Fig. 10—A schematic diagram of the nature of the electrical interaction between the positively charged plasma cloud and (*a*) copper ions and (*b*) the negatively charged surface active species.

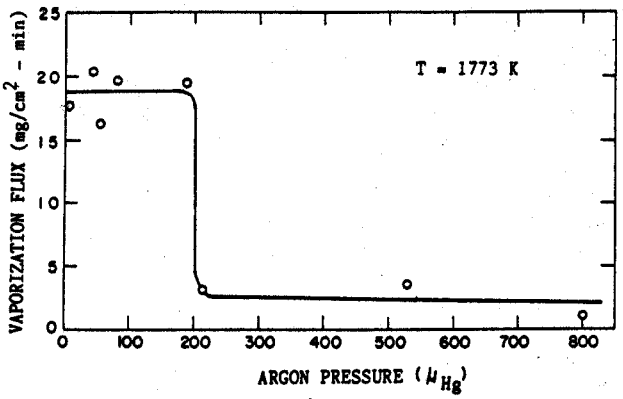

Fig. 11—Variation of vaporization flux of copper in the presence of argon plasma as a function of chamber pressure.

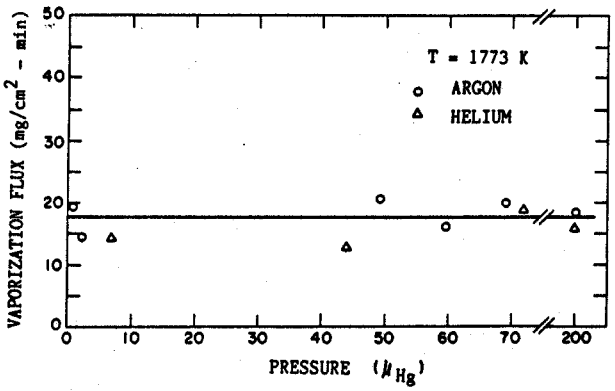

Fig. 12—Variation of vaporization flux of copper as a function of chamber pressure in the absence of plasma under various gases.

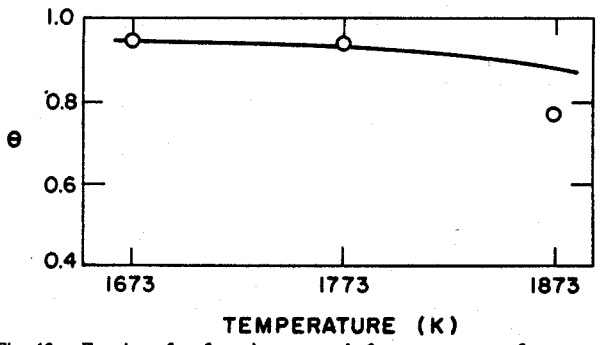

Fig. 13—Fraction of surface sites covered, θ, *vs* temperature for copper-oxygen-sulfur system.

IV. CONCLUSIONS

The rates of vaporization of alloying elements during laser welding of a high manganese stainless steel under various shielding gas environments were found to be independent of both the flow rate and the nature of the shielding gas. The gas phase mass transfer did not contribute significantly to the overall vaporization of alloying elements. Analysis of the numerically computed fluid flow field and independently measured concentration profiles of the vaporizing species near the rapidly cooled weld pool surface indicated that the transport of the alloying elements in the weld pool was rather fast and the transport step did not provide any significant resistance to the alloying element loss. The presence of plasma reduced the vaporization rate of pure copper drops. The experimentally determined vaporization rates of copper in the absence of plasma were in fair agreement with the theoretical vaporization rates calculated from the Langmuir-Knudsen equation incorporating the surface segregation effects due to the presence of small amounts of sulfur and oxygen. The rate of vaporization of alloying elements during laser welding of stainless steels was controlled by plasma influenced intrinsic vaporization at the weld pool surface.

APPENDIX

Equilibrium Vapor Pressure Data Used for the Calculations

The equilibrium vapor pressures of the various vaporizing species, *viz.*, Fe, Mn, Cr, and Ni, over the respective pure liquids expressed in N/m^2 were calculated using the following equation:

$$\log P_{Fe} = -24.609 \times 10^3/T - 8.321 \log T + 0.6686 \times 10^{-3}T - 0.305 \times 10^{-7}T^2 + 38.003 \quad \text{(Reference 11)} \quad [A1]$$

The vapor pressure of manganese at temperatures less than 2900 K is given by the following equation:

$$\log P_{Mn} = -5.58 \times 10^{-4}T - 1.503 \times 10^4/T + 12.609 \quad \text{(Reference 12)} \quad [A2]$$

At temperatures greater than 2900 K, the vapor pressure of manganese was computed from the following equations:

$$\log P_{Mn} = -27.936 \times 10^3/T - 60.675 \log T + 16.026 \times 10^{-3}T - 16.589 \times 10^{-7}T^2 + 193.002 \quad \text{(Reference 11)} \quad [A3]$$

$$\log P_{Cr} = -13.505 \times 10^3/T + 33.658 \log T - 9.290 \times 10^{-3}T + 8.381 \times 10^{-7}T^2 - 87.077 \quad \text{(Reference 11)} \quad [A4]$$

$$\log P_{Ni} = -3.519 \times 10^3/T + 74.940 \log T - 18.042 \times 10^{-3}T + 15.140 \times 10^{-7}T^2 - 214.297 \quad \text{(Reference 11)} \quad [A5]$$

Calculation of Occupied Surface Sites, θ

The fractions of surface sites occupied by the surface active elements at various temperatures were determined from the interfacial tension data as a function of composition and temperature of the melt. Since it is difficult to obtain interfacial tension data at all temperatures and compositions required for the calculations, a formalism to predict interfacial tension data based on the works of Belton[17] and Sahoo[18] was used. Belton used a combination of Gibbs and Langmuir adsorption isotherms to develop the following equation which describes the interfacial tension of a liquid metal in the presence of a surface active element:

$$\gamma^\circ - \gamma = R'T\Gamma_s \ln[1 + Ka_i] \quad [A6]$$

where γ is the surface tension of the solution, γ° is the surface tension of pure metal at the temperature of interest, R' is the gas constant, Γ_s is the surface excess at saturation, K is the adsorption coefficient, and a_i is the activity of species i in solution. Sahoo[18] expressed K, the adsorption coefficient, in terms of an entropy factor and the standard heat of adsorption in the following form:

$$K = \exp\left(\frac{-\Delta S^\circ}{R}\right)\exp\left(\frac{-\Delta H^\circ}{RT}\right) = K_1 \exp\left(\frac{-\Delta H^\circ}{RT}\right) \quad [A7]$$

and expressed the interfacial tension for pure metal, γ°, explicitly as a function of temperature to obtain the following relation between interfacial tension and temperature:

$$\gamma = \gamma_m - A(T - T_m) - R'T\Gamma_s \cdot \ln\left[1 + K_1 a_i \exp\left(\frac{-\Delta H^\circ}{RT}\right)\right] \quad [A8]$$

where γ_m is the surface tension of pure metal at melting point and T_m is the melting point of the pure metal. The values of the five constants used in the above equation for iron-oxygen and copper-oxygen systems obtained from Sahoo's work are provided in Table II. The AISI 201 sample contained 0.004 wt pct S and 0.004 wt pct O. For the calculation of θ, surface tension data for iron-oxygen systems at 0.004 wt pct S concentration are necessary at various temperatures and oxygen concentrations. Since the effect of oxygen on the interfacial tension of iron is more than the effect of sulfur,[17] the interfacial tension data for the iron-oxygen-sulfur system was taken to be approximately equal to that for the iron-oxygen system. The physical modeling experiments were conducted with electrolytic grade copper which contained 0.003 wt pct S and 0.055 wt pct O. Sulfur reduces the interfacial tension of copper more than oxygen when both the impurities are present in equal amounts.[19] However, in view of the fact that the oxygen concentration was about 20 times the concentration of sulfur, the interfacial tension data for the copper-oxygen-sulfur system was approximated to be equal to the data for the copper-oxygen system. Thus, the interfacial tension data[18] for copper-oxygen and iron-oxygen at a given concentration of sulfur was used to prepare a plot of the interfacial tension as a function of $\ln[a_S \cdot a_O^2]$. The surface excess values are obtained from the slope of the plot, $(-R'T\Gamma)$, at various concentrations, and the values of θ at a given concentration are obtained from the ratio of Γ/Γ_s, where Γ_s is the surface excess at saturation. For the Fe-Cr-C and Fe-Si-C systems, Belton[20] has shown that a plot of interfacial tension *vs* $\ln[a_B \cdot a_C]$ where B is Cr or Si can be used to obtain the surface excess values. It is assumed for the calculations presented in this paper that oxygen and sulfur exist on the surface of the melt in the form of SO_2. The calculated values of fraction of surface sites occupied by the solutes, θ, are approximate. However, the calculations demonstrate that a significant portion of the surface sites is occupied by the solutes.

Table II. Constants Used in Equation [A8] for Extrapolation of Surface Tension Data for Iron-Oxygen and Copper-Oxygen Systems (Reference 18)

	Fe-O	Cu-O
γ_m, N/m	1.943	1.382
A, N/(m K)	0.43×10^{-3}	0.27×10^{-3}
Γs, Kg moles/m^2	2.03×10^{-8}	5.30×10^{-9}
K_1	0.0138	0.3295
ΔH°, cal/mole	−35000	−41270

NOMENCLATURE

A	Temperature coefficient of surface tension of pure metal, N/m K
$J_i(T)$	Flux of species i, moles/(cm^2 sec)
K_1	Constant
M_i	Molecular weight of species i, gm/mole
$P_i(T)$	Partial pressure of species i over the alloy at T K, atm
r	Radius of the weld pool, cm
R′	Gas constant, 8.314×10^3 Kg m^2/(s^2 Kg mole K)
R	Gas constant, 1.987 cal/(mole K)
T	Temperature, K
$\dot{v}$	Vaporization rate, gms/sec
γ	Surface tension of the solution, N/m
γ°	Surface tension of pure metal, N/m
γ_m	Surface tension of pure metal at melting point, N/m
θ	Fraction of surface sites occupied by a surface active element
ΔH°	Standard heat of adsorption, cal/mole
Γ	Surface excess of species i, Kg moles/m^2
Γ_s	Surface excess of species i at saturation, Kg moles/m^2

ACKNOWLEDGMENT

This work was sponsored by the United States Department of Energy, Office of Basic Energy Sciences, Division of Materials Science under grant number DE-FG-02-84ER-45158.

REFERENCES

1. D. B. Snow and E. M. Breinan: United Technologies Research Center, Connecticut, ONR report, #R78-911989-14, July 1978.
2. D. W. Moon and E. A. Metzbower: *Welding Journal Research Supplement*, 1983, vol. 62, pp. 53-58.
3. L. R. Hettche, E. A. Metzbower, J. D. Ayers, and P. G. Moore: *Naval Research Reviews*, 1981, vol. 28, pp. 4-20.
4. E. A. Metzbower: *Naval Engineers Journal*, Aug. 1981, pp. 49-58.
5. N. Rykalin, A. Uglov, and A. Kokora: *Laser Machining and Welding*, Mir Publishers, Moscow, 1976, p. 226.
6. P. A. A. Khan and T. DebRoy: *Metall. Trans. B*, 1984, vol. 15B, pp. 641-44.
7. A. Paul and T. DebRoy: *Advances in Welding Science and Technology*, S. A. David, ed., ASM, Metals Park, OH, 1986, pp. 29-33.
8. P. A. A. Khan and T. DebRoy: The Pennsylvania State University, unpublished research, 1986.
9. G. H. Geiger and D. R. Poirier: *Transport Phenomena in Metallurgy*, Addison-Wesley Publishing Company, Inc., 1973, pp. 463-67.
10. A. Block-Bolten and T. W. Eagar: *Metall. Trans. B*, 1984, vol. 15B, pp. 461-69.
11. R. E. Honig and D. A. Kramer: *Physicochemical Measurements in Metal Research*, Interscience Publishers, New York, NY, 1970, vol. 4, pp. 505-17.
12. R. Hultgren, P. D. Desai, D. T. Hawkins, M. Gleiser, K. K. Kelley, and D. D. Wagman: *Selected Values of the Thermodynamic Properties of the Elements*, ASM, Metals Park, OH, 1973, pp. 6-7.
13. A. Paul: Ph.D. Thesis, Department of Materials Science and Engineering, The Pennsylvania State University, 1987.
14. P. Sahoo and T. DebRoy: *Metall. Trans. B*, 1987, vol. 18B, pp. 597-601.
15. F. D. Richardson: *Physical Chemistry of Metals in Metallurgy*, Academic Press, London, 1973, vol. 2, p. 447.
16. P. Kozakevitch: *Surface Phenomena of Metals*, S.C.I. Monograph No. 28, 1968, p. 223.
17. G. R. Belton: *Metall. Trans. B*, 1976, vol. 7B, pp. 35-42.
18. P. Sahoo, T. DebRoy, and M. J. McNallen: *Metall. Trans. B*, in press.
19. K. Monma and H. Suto: *Trans. JIM*, 1961, vol. 2, pp. 148-53.
20. G. R. Belton: *Metall. Trans.*, 1972, vol. 3, pp. 1465-69.